

AUTOMATIC CLASSIFICATION OF *Kepler* THRESHOLD CROSSING EVENTS

SEAN MCCAULIFF³, JON M. JENKINS¹, JOSEPH CATANZARITE², CHRISTOPHER J. BURKE², JEFFREY L. COUGHLIN², JOSEPH D. TWICKEN², PETER TENENBAUM², SHAWN SEADER², JIE LI², MILES COTE¹

Submitted to ApJ

ABSTRACT

The *Kepler* Science Operations Center detects interesting, exoplanet transit-like signals while searching over 211,000 distinct light curves. The mission has produced four catalogs of interesting objects with planet transit-like features known as *Kepler* Objects of Interest (KOI). The total number of objects with transit-like features identified in the light curves has increased to as many as 18,000, just examining the first three years of data. This number of significant detections has become difficult for human beings to inspect by eye in a thorough and timely fashion. In order to accelerate the process by which new planet candidates are classified and to provide an independent assessment of planet candidates, we propose a machine learning approach to establish a preliminary list of planetary candidates ranked from most credible to least credible. The classifier must distinguish between three classes of detections: non-transiting phenomena, astrophysical false positives, and planet candidates. We use random forests, a supervised classification algorithm, that has an error rate of 1.34% with some qualifications.

Keywords: astronomical databases: miscellaneous, binaries: eclipsing, catalogs, methods: statistical, planets and satellites: detection, techniques: photometric

1. INTRODUCTION

The *Kepler* spacecraft is a single instrument spacecraft that maintains its pointing at the designated field almost constantly in order to collect the most contiguous and long running photometric time series possible. While operating, *Kepler* can simultaneously observe approximately 170,000 stars. Data gaps on the order of days result from a monthly data down link and a quarterly 90-degree roll used to maintain the orientation of the solar panels. This roll causes the vast majority of stars to be observed by a different CCD every three months with a one year cycle.

The *Kepler* science processing pipeline (Jenkins et al. 2010a) takes as input raw long cadence pixel data and performs the following steps: calibration, photometry, systematic error correction, transiting planet search (TPS), and transiting planet model fitting (DV). The pipeline produces a list of threshold crossing events (TCE). A TCE is a sequence of transit-like features in the light curve of a given target star that sufficiently resembles the signature of a transiting planet that it merits consideration as such.

TCEs are then subjected to a vetting process performed by the *Kepler* TCE Review Team (TCERT). An initial stage of vetting, known as triage, partitions the set of TCEs into problematic light curves that have instrumental noise and *Kepler* Objects of Interest (KOIs). This is performed by individuals manually inspecting light curves and detection statistics. A KOI is a TCE that contains convincing transit like features that make it likely the TCE is caused by a transiting object and

has not presented any obvious evidence to the contrary. KOIs are further scrutinized with *Kepler* data in later stages of vetting to identify significant evidence that the signal results from an eclipsing binary. TCEs that do not present such evidence are disposed as planet candidates (PC). The vetting process is described in greater detail in Batalha et al. (2013); Burke et al. (2014).

We propose to automate this process of classifying TCEs into one of three classes: planet candidate (PC), astrophysical false positives (AFP) and non-transiting phenomena (NTP). PCs are those KOIs that are confirmed planets, statistically validated planets, or determined to be a planet candidate by the TCERT. AFPs are those KOIs that have been shown to be eclipsing binary stars or have shown evidence that the transiting object being detected is not located around the target star. The class NTP are those TCEs that failed triage.

We use a machine learning algorithm known as the random forest (Breiman 2001) to find a function that maps attributes produced by the *Kepler* Pipeline for each TCE to a classification of PC, AFP or NTP. This classification function is purely based on the statistical distributions of the attributes for each TCE (e.g. SNR of the transit model fit) with respect to TCEs classified in the manual vetting process. These algorithms do not attempt to physically model the process of planet transits beyond what is already present in the TCE attributes. Random forests have been applied to a variety of classification problems, perhaps closest to this problem is that of classifying variable stars Dubath et al. (2011) and Richards et al. (2011).

The paper is organized as follows. In section 2 we give an overview of the relevant portions of the *Kepler* pipeline that generate the inputs to the random forest. Section 3 introduces notation and describes the rationale behind the random forest algorithm. In section 4 we discuss the provenance of our data and the source of our

sean.d.mccauliff@nasa.gov

¹ NASA Ames Research Center, Moffett Field, CA 94035, USA

² SETI Institute/NASA Ames Research Center, Moffett Field, CA 94035, USA

³ Orbital Sciences Corporation/NASA Ames Research Center, Moffett Field, CA 94035, USA

known class labels. Section 5 talks about how we have pruned our set of attributes and which attributes turned out to be the most important. Section 6 contains an analysis of the classification performance and a comparison to reference classification algorithms on the same data set. A survey for transiting planets will initially discover larger, shorter period planets before discovering smaller, longer period planets so that the training set will lag in period behind the unknown data. Section 7 discusses issues involving how the automated classification would be applied to an exoplanet transit survey. Finally, section 8 talks about future work we may perform to assist in discovering additional transiting exoplanets as well as to improve the performance of the classifier.

2. *Kepler* PIPELINE

2.1. *Kepler* light curves

Photometric data are composed of a set of co-added 6 second integrations with a readout time of 0.5 seconds whose durations total 29.4 minutes. Co-added pixel values, from fields around approximately 170k target stars, are downloaded from the spacecraft; the remainder of the processing is performed on Earth. A full 29.4 minute co-add is known as a long cadence. This paper concerns itself only with long cadence data. After calibration, light curves are produced using simple aperture photometry and subjected to cotrending to remove systematic noise (Smith et al. 2012; Stumpe et al. 2012).

2.2. *Transiting Planet Search*

The *Kepler* Pipeline (Jenkins et al. 2010a) is a data reduction pipeline used for translating the *Kepler* raw pixel data into potential transiting planet detections. In particular, this paper concerns itself with the last two modules of the pipeline; those that identify threshold crossing events (TCEs) and their subsequent transit model fitting. The *Transiting Planet Search* (TPS) (Jenkins et al. 2010b) module takes as input the systematic error-corrected light curve for a star; searches a parameter space of possible transit signatures; and outputs a TCE or says that one does not exist on the target star. This produces a smaller list of stars that have TCEs. This subset of target stars is then given to the *Data Validation* (DV) module. DV fits this initial TCE to a transit model using the geometric transit model described by Mandel & Agol (2002) with the limb-darkening coefficients of Claret & Bloemen (2011). DV then gaps the transit signature from the light curve and uses TPS to find additional TCEs on the same target star. This process repeats until no more TCEs are found on a star or a processing timeout has been reached.

The TPS algorithm detects transit-like signatures in a whitened light curve by using a wavelet matched filter. It is a matched filter in the sense that a reference transit pulse is whitened in the same manner as the light curve before being convolved with the whitened data. TPS searches a parameter space of varying transit duration ($D \in \{1.5, 2.0, 2.5, 3.0, 3.5, 4.5, 5.0, 6.0, 7.5, 9.0, 10.5, 12.0, 12.5, 15.0\}$ hours). This produces a Single Event Static (SES) time series that is the significance of the detection of the reference transit pulse centered on that particular time for each D . This is computed as $SES(t) = \mathbb{N}(t)/\sqrt{\mathbb{D}(t)}$, where $\mathbb{N}(t)$ is the correla-

tion time series; that is, how well the reference transit pulse correlates with the light curve. $\sqrt{\mathbb{D}(t)}$ is the expected signal to noise ratio of a signal that exactly matches the template pulse. The Combined Differential Photometric Precision (CDPP) is $1E6/\sqrt{\mathbb{D}(t)}$ ppm. TPS then constructs a Multiple Event Statistic (MES) that characterizes a significant detection in a search over varying orbital periods p and epochs t_0 by folding $\mathbb{N}(n)$ and $\mathbb{D}(n)$. A $MES > 7.1\sigma$ may produce a TCE if it also passes additional statistical tests described by Seader et al. (2013). If several permutations of (t_0, p, D) would produce a TCE, then TPS only reports the event with the maximum MES as the TCE for the target star. TPS-generated diagnostics such as MES and SES are the basis of some of the classifier attributes (see section 5.3). The minimum MES, which can be negative if the light curve is anti-correlated with the reference transit pulse, is also computed by TPS. This is referred to as the MES_{min} . An event with a negative MES_{min} would look like a repeated brightening above the median flux.

In addition to detecting PCs and AFPs, TPS often generates a threshold crossing event for NTPs. NTPs are caused by instrumental, systematic noise (Caldwell et al. 2010), and stars with high variability such as “heartbeat” stars (Thompson et al. 2012). Many NTPs have periods with approximately one year in duration as the electronics associated with the instrumental signatures rotates back into the same observing field. Unfortunately, this part of parameter space corresponds to the habitable zone of Sun-like stars.

2.3. *Data Validation*

Data Validation (DV) (Wu et al. 2010) is a set of algorithms that perform tests to determine the suitability of the TCE as a planet candidate. In particular, DV fits the transiting portion of the light curve to a transit model using the geometric transit model described by Mandel & Agol (2002) with the limb-darkening coefficients of Claret & Bloemen (2011) and constructs a set of diagnostic tests to help determine the nature of the TCE. DV also attempts to locate the actual source of the transits (Bryson et al. 2013), in order to determine if the actual transit signal is being induced by a source offset from the target star. This can be caused by background eclipsing binaries (BEB), optical ghosts of bright stars with periodic signatures, or other unresolved contamination (Coughlin et al. 2014). DV constructs difference images between the in-transit and out-of-transit images for the target. The centroid of the difference image is then the center of the transit source. If the difference image is significantly offset from the out-of-transit centroid, then a background eclipsing binary may have produced the transit-like signal. Using the transit centroid offset from the position of the target star in the *Kepler* Input Catalog (KIC) or the out-of-transit centroid offset turns out to be useful for detecting AFPs (section 5.3).

3. RANDOM FORESTS

3.1. *Introduction*

A random forest itself is an ensemble of decision trees. Each tree votes for the classification of an unknown object based on a vector of attributes that describe the object in question. The classification the forest assigns

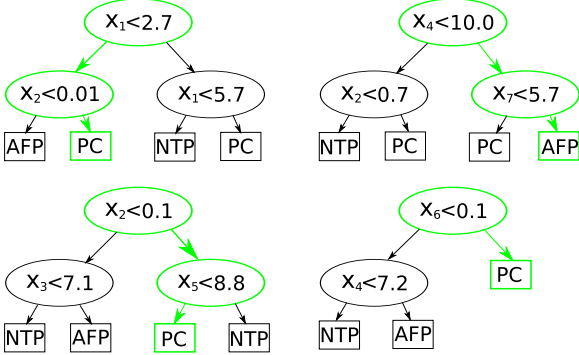


Figure 1. A hypothetical, simplified random forest. Left branches are taken if the inequality is satisfied otherwise the right branch is taken. A TCE with the attribute vector of $x = (2, 0.2, 4, 11, 5, 0.3, 6.1)$ is classified. Bold, green lines indicate paths taken in the decision trees. The individual decision trees have voted { PC, AFP, PC, PC } yielding a classification of PC. A decision tree is a directed graph where each internal vertex in the graph is a binary test; in this case, the tests are inequalities. If the test is true then one branch is taken else the other branch is taken. Leaf vertices indicate classifications. The trees in the random forest are constructed in such a way that attributes under test are randomly selected and so each tree makes a different set of tests. Figure 1 shows a simplified, hypothetical random forest.

3.2. Notation

\mathbf{X} is the set of random variables that describe a TCE. Sometimes we refer to \mathbf{X} as the attributes of the TCE. When we need to refer to a particular random variable without naming it, we use x_i or some other subscript. So $\mathbf{X} = \{x_1, \dots, x_A\}$. A is the number of attributes or $|\mathbf{X}|$. The instantiation of the set of all the random variables for all the TCEs under consideration is X . When referring to the set of instantiations for a particular TCE we use x . s refers to a constant that is used to split X into two different subsets. s_i is a split on the i th attribute. \mathbf{Y} refers to the set of all classes to which a TCE might belong; these are sometimes known as labels. A particular label is denoted $y_i \in \mathbf{Y}$ and there are $C = |\mathbf{Y}|$ distinct classes. For this classification problem, $\mathbf{Y} = \{y_1, y_2, y_3\} = \{PC, AFP, NTP\}$. Y refers to the instantiation of all the labels for all the TCEs under consideration. y is the instantiation for a particular TCE (usually in the training set). \mathcal{L} is a set of instantiations of all the attributes X and their labels Y ; that is, attributes that describe all the TCEs and the TCEs’ labels. \mathcal{L} is also known as the training set. The size of the training set is $N = |\mathcal{L}|$; the number of labeled TCEs.

The purpose of classification is to assign an estimated label, \hat{y} , given an instantiation of attributes x . A classification function generates a prediction for a set of attribute instantiations, $h : x \rightarrow \hat{y}$. Finally, an importance function returns an estimate the importance of an attribute relative to other attributes, $Q : x_i \rightarrow \mathbb{R}$. Sometimes we want to refer to the class-conditional importance $Q(x_i|y_j) \rightarrow \mathbb{R}$; that is we want to measure how important a variable is to predicting a particular class rather than the importance over all classes.

3.3. Decision Trees

As an example, equation 1 is a simple, makeshift, classification function. The training set consists of only three attributes to describe a TCE and two splits.

$$h(MES_{min}, MES_{max}, \Delta_{centroid}) = \begin{cases} \text{classify TCE as NTP, if } \frac{MES_{max}}{MES_{min}} < s_1 \\ \text{classify as PC, if } \Delta_{centroid} < s_2 \\ \text{classify as AFP, otherwise} \end{cases} \quad (1)$$

$\Delta_{centroid}$ is the difference between the star’s *Kepler* Input Catalog (KIC) position and its mean out-of-transit centroid in arc seconds. MES_{min} is the minimum, multiple event statistic discovered by the TPS; indicating repeated events above the baseline stellar flux. MES_{max} is the highest multiple event statistic discovered by TPS. A TCE representing a strong transit detection should have a high ratio of these two attributes. This is attribute 2 in section 5.3. TCEs caused by BEBs should show an offset from their KIC position, so a high $\Delta_{centroid}$ value is cause to classify a TCE as an AFP.

Optimizing the parameters s_1, s_2 for the minimal misclassification rate of h yields a misclassification error rate of 0.0886. The misclassification error rate is simply the number of incorrect classifications divided by the size of the training set (N). A logical next step to reduce the error rate would be to consider additional attributes that would discriminate TCEs. The Classification and Regression Tree (CART) algorithm (Breiman et al. 1984) can construct a recursive nesting of conditional tests of arbitrary depth. These are sometimes visualized as a tree of conditionals called a decision tree. When building a decision tree, CART minimizes the following function for all splits s_i under consideration:

$$\Delta \mathbf{I}(\mathcal{L}, s) = |\mathcal{L}| \mathbf{I}(\mathcal{L}) - |\mathcal{L}_{x_i < s}| \mathbf{I}(\mathcal{L}_{x_i < s}) - |\mathcal{L}_{x_i \geq s}| \mathbf{I}(\mathcal{L}_{x_i \geq s}). \quad (2)$$

$P(y_i)$ is the frequency of class y_i in \mathcal{L} . Function \mathbf{I} is an impurity function ($\mathbf{I} : \mathcal{L} \rightarrow \mathbb{R}$) chosen so that it is maximum when all $P(y_i)$ are approximately equal and zero when any $P(y_i) = 1$. $\mathcal{L}_{x_i < s}$ is the subset of \mathcal{L} consisting of the training examples where attribute x_i is less than the threshold s . The members of $\mathcal{L}_{x_i < s}$ depends only on the ordering of the attributes relative to the split. This implies attribute transformations that are class independent and do not change the ordering of training examples will result in the same $\mathcal{L}_{x_i < s}$. For example, $\log x_i$ would not change the results of any splits. When CART is selecting a split for the training set, it iterates over all x_i to find the attribute with the largest $\Delta \mathbf{I}$.

One possible definition for \mathbf{I} is an information function:

$$\mathbf{I}_Z(\mathcal{L}) = - \sum_{i=1}^C P(y_i|\mathcal{L}) \log_2 [P(y_i|\mathcal{L})]. \quad (3)$$

So that when when a split is selected using equation 2 we are maximizing the information loss of the split. A perfect split would result in the members of $\mathcal{L}_{x_i < s}$ and

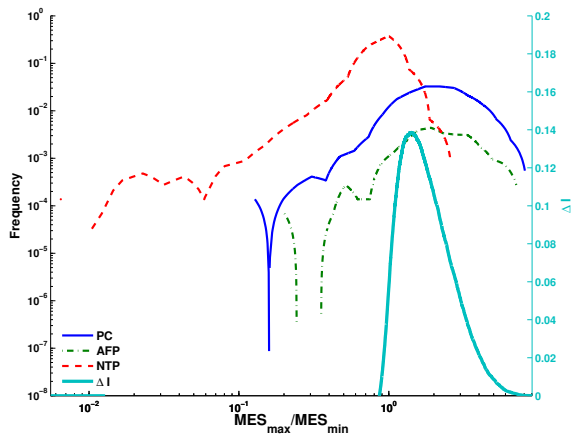


Figure 2. $\Delta\mathbf{I}$ computed using impurity function \mathbf{I}_G for MES_{max}/MES_{min} over the entire training set. We would split the training set at the maximum of $\Delta\mathbf{I}$.

$\mathcal{L}_{x_i > s}$ being of the same class and therefore all information would have been lost.

In practice the Gini impurity function:

$$\mathbf{I}_G(\mathcal{L}) = \sum_{i=1}^C P(y_i|\mathcal{L})[1 - P(y_i|\mathcal{L})] \quad (4)$$

\mathbf{I}_G , is used since it is faster to compute and usually results in the same split. \mathbf{I}_G is the sum of the misclassification probabilities. That is, the probability of guessing class \mathbf{y}_i for some example in \mathcal{L} , when the label is actually some other class. Breiman et al. (1984) discusses other impurity functions. Figure 2 gives an example of $\Delta\mathbf{I}$ evaluated at every possible split. Splitting the training set occurs between the attribute values with the maximum $\Delta\mathbf{I}$.

Splitting the training set happens recursively so that $\mathcal{L}_{\mathbf{x}_i < s}$ and $\mathcal{L}_{\mathbf{x}_i > s}$ are then the training set for the next level of the decision tree. Tree construction ends when a split would result in a training set with instances of only a single class; impurity has fallen to zero. This generates the leaf vertex that assigns a class \hat{y} to x when the tree is evaluated.

3.4. Random Forest Description

The forest is a set of base, decision tree classifiers $\{h_1, \dots, h_k, \dots, h_{N_{tree}}\}$. Each tree, $h_k(\mathbf{x})$, is trained on \mathcal{L}_k which is a bootstrap replica of \mathcal{L} known as a bag. Each bag is about 2/3 the size of the training data set. The observations not contained in the bag, $\overline{\mathcal{L}}_k$, are known as the out-of-bag data (OOB). The number of trees N_{tree} is one of two tunable parameters for this algorithm. For this problem we use $N_{tree} = 15,000$. Each tree's misclassification error can be evaluated on its OOB data to provide an unbiased estimate of the misclassification error of the random forest. Unlike other classification algorithms, this allows us to use the entire training data set rather than cross-validation.

Attributes can be ranked by their importance; a measure of how much the attribute influences the error rate of the random forest. This is computed by using the OOB data, permuting the values of the attribute among the OOB TCEs and recomputing the error rate for the tree. The importance is then the mean increase in error over all the trees in the random forest when the value of the attribute has been permuted. Random permutations are

used so that values come from the same distribution, but are no longer correlated with any classes. We use the importance in section 5 to prune the number of attributes in our training set.

Unlike any individual decision tree the random forest has the nice property of having bounded error. That is, the overall misclassification error converges to this error bound. In order to prove this, Breiman (2001), makes the assumptions that individual trees make their decisions independently of other trees. When a split is made during the construction of h_k , a random subset of attributes are considered for the split rather than all attributes. m_{try} is the number of attributes to select randomly during a split. These two techniques (i.e. bootstrap sampling and choosing a random subset of attributes at each split) break the correlation among the decision trees in the forest so that they approach the ideal of independent classifiers.

The random forest's error is bounded by the equation,

$$Err_{RF} \leq \bar{\rho}(1 - g^2)/g^2. \quad (5)$$

where g is the strength of the the random forest. This is the average difference between the proportion of votes for the correct class and the maximum proportion of votes for any other class over all of \mathcal{L} . $\bar{\rho}$ is the correlation among all the pairs of trees of the random forest over all of \mathcal{L} after function

$$R(k) = \begin{cases} 1, & h_k(x) = y \\ -1, & h_k(x) = \text{the most common misclassification of } x \\ 0, & \text{otherwise} \end{cases}, \quad (6)$$

has been applied to the classification of each tree on the training data.

The error bounds of the random forest then depend on how correlated the decisions of the trees are with each other and how well the forest as a whole separates between the correct class and the next best classification. Breiman (2001) contains a proof for convergence of the random forest to these error bounds.

4. DATA SET

4.1. TCE Catalog

The TCE catalog used is from the first twelve quarters of Kepler data, described by Tenenbaum et al. (2013). This TCE catalog contains a total of 18,407 TCEs. The TCE ephemerides are correlated with the ephemerides of known planets, planet candidates and astrophysical false positives from the NASA Exoplanet Archive⁴. We use the cumulative KOI catalog that was available on the date 2013 June 25 for the training data ephemerides. In this particular run of the *Kepler* pipeline, 2,126 targets that generate TCEs were excluded from consideration. The majority of these excluded stars are known eclipsing binaries from the Prša et al. (2011) catalog. Planets that have very short periods and relatively deep transits are identified as harmonics and are removed by TPS (e.g. Kepler-10b (Batalha et al. 2011)). These are not

⁴ <http://exoplanetarchive.ipac.caltech.edu>

accounted for in the TCE catalog since they are not found by the *Kepler* pipeline. Planets with large transit timing variations and planets whose existence can only be inferred by transit timing variations (e.g. Kepler-19b,c (Ballard et al. 2011)) are also not in the TCE catalog. There are some cases where TPS has identified multiple TCEs for a single eclipsing binary. When this occurs, the TCEs usually have a period that is an integer multiple of an accompanying TCE on the same target star. No attempt is made to match these TCEs to the source eclipsing binary and so they are considered unlabeled and not used in the training set.

4.2. Non-Transiting Phenomena

For quarter one through quarter twelve of the *Kepler* data, the TCERT reviewed all of the TCEs that were not caused by previously known KOIs. Each TCE was examined by two or more people (vetters) to see if it had one of the following problems: stellar variability, instrumental effects, or anomalous behavior. A TCE is considered a product of stellar variability if it shows sinusoidal activity especially outside of the primary transit event. Instrumental noise is defined as a TCE exhibiting a transit-like signature apparently caused by spacecraft systematics, such as those induced by periodic spacecraft operations and uncorrected transient events such as cosmic ray hits. In some cases anomalous TCEs occur if there was insufficient data to make a classification, or if the transit did not appear at the expected position in the light curve. This step in the process of TCE vetting is known as triage. For examples of NTP in our training set, we only consider TCEs where there was a unanimous decision among all the TCERT vetters that examined the TCE under consideration had one or more of the problems disqualifying it as a new KOI. This yields 11,304 TCEs that are in the class NTP. Since these were TCEs discovered from the pipeline run, their ephemerides did not require matching against a known catalog.

More information about the TCERT process can be found in Batalha et al. (2013); Burke et al. (2014) and Rowe (in preparation).

4.3. Planet Candidates and Astrophysical False Positives

Our training set for class PC and AFP are derived from the public *Kepler* Objects of Interest (KOI) catalog maintained by the NASA Exoplanet Archive. This is the union of many KOI catalogs, described in more detail in Borucki et al. (2011); Batalha et al. (2013); Burke et al. (2014) and Rowe (in preparation). A KOI can be a confirmed or validated exoplanet (confirmed or validated by one of several methods), a planet candidate (PC), an astrophysical false positive (AFP), or undispositioned. A PC has a convincing transit-like signature in the light curve for the target star, but may lack additional information needed to confirm it as an exoplanet. Confirmed and statistically validated planets are also in the class PC. The class of AFP includes eclipsing binaries, background eclipsing binaries and unresolved contamination from other astrophysical sources. We drop undispositioned KOIs from the training set and consider them unknown. About eight of the PCs have been corrected to AFPs with information that was available at a later date.

After ephemeris matching our training set has 2,879 PCs and 393 AFPs. This probably underrepresents the true population of AFPs since many AFPs were excluded from our pipeline run (see section 4.1).

4.4. Matching Ephemerides

We match the ephemeris contained in the KOI catalog to the TCE catalog in order to identify labels for training data. Additionally, this algorithm is also used to compute correlations with other TCEs. This turns out to be an important attribute for class AFP and NTP (section 5).

The KOI catalog and the TCE catalog contains an ephemeris which we defined as the tuple (C, t_0, p, D) for each entry in the catalog. Where C is the KIC catalog identifier, t_0 is the epoch, p is the orbital period, and D the transit duration. \mathbf{K} and \mathbf{J} denote sequences of tuples for their respective catalogs KOI and TCE. An ephemeris matching function is then $m : (\mathbf{K}, \mathbf{J}) \rightarrow \mathbf{K} \times \mathbf{J}$. Our ephemeris matching function also requires additional parameters that specify the observing window, t_{start} and t_{end} .

If a transit occurs during a data gap, such as a safe mode, it will be missed in the raw data. For the purpose of ephemeris matching, we want to represent all the transits that could have occurred during the observing window, so we adjust the relative epoch to correspond to the first transit that could have occurred after the start of the observing window, in case the first transit was missed due to a data gap. For each KOI $K_k \in \mathbf{K}$, and each TCE $J_j \in \mathbf{J}$, we replace the epoch with the relative epoch, which is the time relative to the start of the observing window expressed as:

$$t'_0 = t_0 - p[\arg \max_a \{x = t_0 - pa | a \in \mathbb{N}_0, x \geq t_{start}\}]. \quad (7)$$

For each KOI K_k , we identify all the TCEs J_j where $C_k = C_j$ (the set of TCEs and KOIs that are on the same target star). We identify the best match to the KOI in the following way. We compute the Pearson's correlation coefficient between the KOI transits and the TCE transits. We construct a discrete transit indicator vector z_k and z_j over the observing window of each KOI. The transit indicator vector takes a value of one during a transit and zero outside of a transit. To compute it, we sample the observing window every 1 minute, which gives a large number of samples during a transit. The sampling time can be made smaller at the expense of computation time.

Each transit indicator vector is normalized by the square root of its sum, so that its dot product with itself is unity. The correlation for the KOI and the best-matched TCE

$$\rho_{match} = \frac{z_k}{\sqrt{\sum z_k}} \cdot \frac{z_j}{\sqrt{\sum z_j}}, \quad (8)$$

is the dot product of their normalized transit indicator vectors.

Evidently from figure 3, a minimum correlation of 0.75 insures that the matched period will never be off by a factor of two. Accordingly, if the ρ_{match} of the best-matched TCE is greater than 0.75, we accept it as a true match. If the best match to a KOI has correlation below

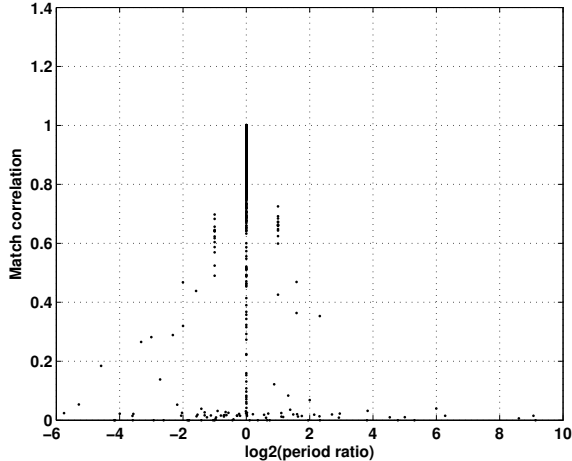


Figure 3. KOI to TCE correlation function vs. KOI to TCE period ratio. The abscissa is \log_2 of the ratio of the period of the KOI to the period of the best-matching TCE. The ordinate is the correlation.

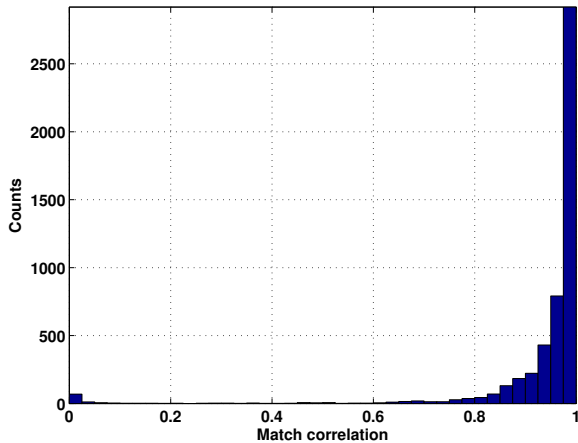


Figure 4. A histogram of the match correlation, showing that the vast majority of KOI matches have correlation near unity.

0.75, the KOI is labeled as unknown and not included in the training set.

5. ATTRIBUTES

5.1. Missing Attribute Values

In some cases attribute values are not available. This can occur because information is missing in stellar catalogs, the DV fit fails to converge, or a processing timeout is reached. Several methods of dealing with missing data were investigated: using sentinel values, imputing missing values and training different classifiers for each subset of missing data. Imputing missing values involves substituting reasonable values for the missing data. During training, class-conditional values of mean, median and most common are used. During prediction the non-conditional version of those functions are used to fill values for the unclassified TCEs. Training multiple classifiers involves identifying those subsets of attributes that commonly have missing values and then training classifiers on those attributes that are defined. A sentinel value is a special value that is not commonly seen

in the distribution of the attribute; we use -1. Using a sentinel value turns out to be the simplest method with the lowest error rate. Internally, when stellar parameters are not available, DV uses the sun’s parameters. For example, when stellar radius is not available DV assumes the unknown radius is $1 R_{\odot}$.

5.2. Attribute Pruning

The initial attribute set contains 237 attributes that are based on the wavelet matched filter used by TPS, transit model fitting, difference image centroids and some additional tests.

The principle of parsimony says we should prefer a classifier that uses fewer attributes to one that uses more attributes. Also, should many attributes have poor strength, that is poor prediction value, then their presence in the training set will cause degradation of classification performance. So, we attempt to remove weak attributes. Attributes that have no correlation at all with the TCE classification can even have negative importance. Their removal will slightly decrease the misclassification rate. Finally, attributes that are correlated with each other can cause the random forest’s error bound to be weaker than it might otherwise be, see equation 5. For these reasons we remove unneeded attributes from our initial training set.

Before our final random forest is trained we train an initial random forest with all the attributes in order to generate their importances, $Q(\mathbf{x}_i)$ (section 3.4). More specifically we are interested in the class-conditional importance $Q(\mathbf{x}_i|\mathbf{y}_c)$. The maximum of all the class conditional importances is $\max_c(Q(\mathbf{x}_i|\mathbf{y}_c))$ for our three class problem this is $\max(Q(\mathbf{x}_i|\mathbf{y}_1), Q(\mathbf{x}_i|\mathbf{y}_2), Q(\mathbf{x}_i|\mathbf{y}_3))$. To drop weak attributes, we trained 151 random forests each with a different randomly generated attribute. The values of this attribute are generated via random number generator and are not correlated with any of the classes. This gives us an estimate of the importance of a random attribute, $Q(\text{random})$. We choose a cutoff of 6σ of $Q(\text{random})$ above zero importance; this turns out to be $5E-5$. Attributes that have a maximum, class-conditional importance less than this threshold are dropped.

Equation 5 implies that removing correlated attributes can decrease the error rate of the random forest. To remove correlated attributes, we compute the correlation matrix, $\rho_{i,j}$, from our matrix of attributes. θ_{ρ} is a correlation threshold, attributes $(\mathbf{x}_i, \mathbf{x}_j)$ whose $\rho_{j,j}$ is greater than this threshold are considered significantly correlated. We drop the attribute that has the lower of the two class-conditional importances $\max_c(Q(\mathbf{x}_i|\mathbf{y}_c))$. To estimate θ_{ρ} we trained a random forest by imposing various values of $\theta_{\rho} \in [0.15, 1.0]$ in 0.05 increments. We verified that the OOB error (section 3.4) differs by only $5E-4$ in the interval $\theta_{\rho} [0.35, 1.0]$. Lower values of θ_{ρ} increase the OOB error. Therefore reducing the attribute correlation threshold does not produce any significant decrease on misclassification error. Although we do not see a large decrease in the error rate this still allows us to reduce the number of attributes used by the random forest.

At the minimum OOB error, $\theta_{\rho} = 0.55$ and there are 77 attributes that meet our thresholds. The ten most important of these attributes are described in detail in section 5.3.

5.3. Most Important Attributes

We discuss the top 10 most important attributes in this section. This cutoff is arbitrary for the sake of brevity. The range of attribute importance of the top 10 attributes is from 7.5% increase in OOB error down to a 5.3% increase in OOB error. For the purpose of ranking attributes by importance we use the maximum of the class-conditional importances.

Figure 5 and figure 6 have the class-conditional, attribute distributions for these attributes.

1. The maximum ephemeris correlation, ρ_{match} , (equation 8) computed for a TCE against all the other TCEs on the same star. If there is only one TCE on the same star then this value is zero. When the ephemerides of TCEs on the same star are highly correlated it is an indication that an secondary eclipse may be present and has been detected as a TCE. For NTPs this may indicate that a similar source of instrumental noise has been detected with a slightly different phase.
2. The absolute value of the ratio of the maximum MES to the minimum MES (see section 2.2) found over all search periods. When this value is near 1 it indicates that the periodic events lower than the median flux are of similar statistical significance to similar events greater than the median flux. This attribute attempts to eliminate TCEs that are problematic with respect to stellar variability and instrumental noise.
3. The SNR for the all-transit model fit. This is the transit depth normalized by the mean uncertainty in the flux.
4. MES scaled by SES auto-correlation statistic; $MES(1 - R)$. The expected SES time series should have negligible auto-correlation strength, R , beyond the transit duration time scale. This expectation is not always met in practice for *Kepler* flux time series having residual astrophysics and systematics remaining after the detrending and whitening filter is applied.

To identify targets with enhanced auto-correlation strength beyond the expectation, we begin with the SES time series assuming a 10.5 hour transit duration and remove cadences with bad data. The remaining good cadences are separated into blocks of 4,250 cadences (similar to a single *Kepler* observing quarter). For each block of 4,250 cadences the auto-correlation is calculated out to lag 1050, and we calculate the fraction of the lags where the auto-correlation value is above or below the 95% or 5% expectation, respectively. We simulate the expected auto-correlation value through 150k Monte Carlo trials. A Monte Carlo trial starts with a random realization of a zero-mean, unit-variance Gaussian vector of length 4,250 with a moving average applied with a 10.5 hour window size. The Monte Carlo trial roughly corresponds to the expectation for the SES time series in the null case. We measure the auto-correlation on the Monte Carlo trials to empirically estimate the 5%

lower and 95% upper bound expectation at each lag.

The expectation for a null result (well behaved) SES time series is an auto-correlation strength of 0.05; meaning 5% of the lags for a typical SES time series are above the expectation set by the Monte Carlo simulation. As values approach 1.0 for the auto-correlation strength, the SES is demonstrating very large amounts of auto-correlation and can violate an underlying assumption of the detection statistics. We use the median of the auto-correlation strength across all the blocks to scale the detection statistic, R .

5. The χ^2 for the all-transit model fit. This is the raw χ^2 value; that is, not scaled by the degrees of freedom.
6. Same as attribute 5, but this only considers the odd numbered transits. Comments about odd and even transits made in attribute 7 apply equally here as well. The Kolmogorov-Smirnov test shows the importance of this attribute is significantly greater than the all-transit-fit version of this attribute (attribute 5) for class NTP with $p \ll 0.001$.
7. The ratio of the fitted planet's semi-major axis to the star radius for only the even numbered transits.

Sampling only the even transits (or conversely the odd transits) may have the effect of skipping or including quarters of data that are more problematic. During the second quarter of operation *Kepler* experienced a number of safe modes causing thermal transients. During the fourth quarter one of the CCDs modules failed. During the eighth quarter a number of safe modes occurred. *Kepler* experienced a coronal mass ejection event during the twelfth quarter.

In order to see if the importance of this attribute was due to the randomness of the random forest we trained 40 random forests and then tested the distributions of the importances for this attribute vs the distribution of the importances of the all-transit-fit version of this attribute. The Kolmogorov-Smirnov test shows the importance of this attribute is significantly greater than the all-transit-fit version of this attribute for class NTP with $p \ll 0.001$.

Additionally we computed the importance of this attribute for every TCE. The TCEs that show this attribute as having higher importance than all-transit-fit version of this attribute tend to have longer periods; greater than 4 days. This also corresponds with the somewhat bimodal distribution of NTPs which tend to be more prevalent at relatively shorter and longer periods as shown in plot of attribute 7 in 6. There is a weak negative correlation of -0.22 (Pearson's correlation coefficient) with the effective temperature of the target star.

8. The angular offset on the plane of the sky between the best-fit centroids from the difference image and the KIC position by averaging over all quarters.

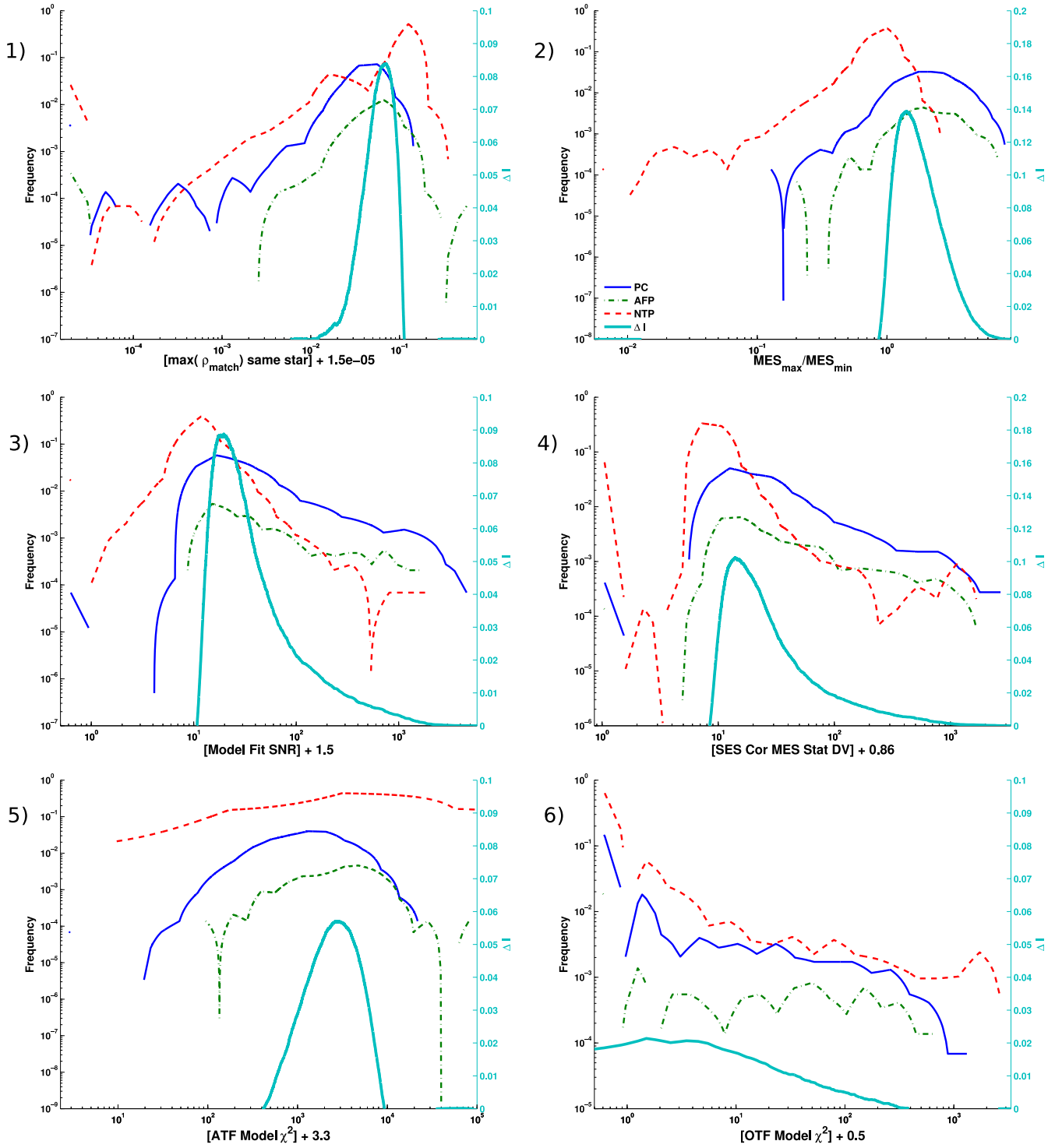


Figure 5. Class-conditional distributions of attributes 1 through 6. If an attribute's domain extends to zero or negative numbers a small constant has been added so that it can be log scaled. ΔI (equation 2) is plotted to show where a split might be made if it was the first split in a decision tree.

The KIC position is subtracted from the difference image centroid. TCEs with large offsets from the KIC position are believed to be caused by background eclipsing binaries or some other events that are not on the target star. This attribute is the uncertainty of this offset not the offset itself.

9. The significance of attribute 8 rather than the uncertainty itself.
10. The proportion of the light curve that was missing during this TCEs transit. We use an already detrended light curve that is median detrended with a window 3 times the transit duration. This is folded on the TCE ephemeris. The detrended light curve is binned with a bin width of half a transit duration for bins within 4 transit durations of the transit center. This attribute is the fraction of the bins that have any data contributing to them. A value of less than one indicates the TCE is overlapping with a region of data that are missing when phase folded on the ephemeris.

6. CLASSIFICATION RESULTS

6.1. Assessment

When assessing classification performance we use the OOB error rather than using cross validation (the common approach for estimating the misclassification rate). We tuned the number of trees in the random forest so that the OOB errors are close to the leave-one-out-cross-validation votes. When $N_{trees} = 1,000$ OOB votes have a correlation with the leave-one-out-cross-validated votes of 0.90. When $N_{trees} = 3,000$ this correlation becomes 0.998. We use $N_{trees} = 15,000$, since this allows us some margin of error and is still computationally tractable. The value of m_{try} suggested by Liaw & Wiener (2002) is $\lceil \sqrt{A} \rceil$, where A is the number of attributes. In practice the random forest is not very sensitive to changes in m_{try} . For our final 77 attributes $m_{try} = 9$.

We are able to achieve OOB error rate of 2.19%. It's possible to stop here and use this vote tuple to assess the performance, but we also weight the votes so they minimize the OOB error. The OOB votes are a tuple $V = (V_{PC}, V_{AFP}, V_{NTP})$, $PC = 1$, $AFP = 2$, $NTP = 3$. Since each TCE used for training is out of bag a random number of times we normalize the votes by the number of trees for which the training TCE was OOB so that $\sum V_x = 1$. The votes are weighted by doing a log space search for the weights ω_2, ω_3 that minimize the OOB error

$$E_{OOB} = \frac{\sum_{i \in \mathcal{L}} I(y_i \neq \arg \max_j V_j \times \omega_j)}{N}. \quad (9)$$

Parameter ω_1 is not a free parameter and is set to 1. The function $I : y \rightarrow 0, 1$, is an indicator function that returns 1 for correct classifications else it returns 0.

At the optimal operating point the random forest is able to achieve E_{OOB} of 1.34%, an improvement of 0.85%. Table 1 describes the precision and recall for each class. Precision is the probability that a classification is correct $P(y = \hat{y} | \hat{y} = y_i)$. Recall is equivalent to detection rate (DR), that is the probability that a class was classified correctly $P(\hat{y} = y_i | y = y_i)$.

Table 1

Random forest precision and recall

Class	Precision	Recall (DR)
PC	95.9%	98.7%
AFP	93.1%	69.0%
NTP	99.5%	99.7%

Table 2

Random forest confusion matrix

Training Set Class	Predicted Class		
	PC	AFP	NTP
PC	2,843	8	28
AFP	98	271	24
NTP	25	12	11,267

From the weighted OOB votes we produce a Receiver Operating Characteristic (ROC) curve that shows detection rate as a function of false positive rate. To generate the curve we calculate the false positive rate at vote thresholds in .01 increments in the interval [0,1]. A vote threshold of one is accepting a detection only when all trees are unanimous and a zero vote threshold is accepting every classification for the class under examination. A vote threshold of zero indicates that an instance of the class will never be misclassified, but guarantees a high false positive rate. The DR is the number of instances of the class correctly classified divided by the number present in the training data. The false alarm rate (FAR) is the number of misclassifications divided by the number of instances of the undesirable classes detected in the training set. The Area Under the Curve (AUC) is the integrated area under the ROC curve. This is a useful metric when comparing classifiers. A classifier with a superior AUC will have some trade off between DR and FAR that results in higher DR/FAR ratio than one with a lower AUC. Figure 7 is the ROC curve showing the trade off between correctly classifying a $PC \cup AFP$ vs accepting a NTP as a $PC \cup AFP$.

Planet candidates vs astrophysical false positives show an orbital period dependent ROC curve, see figure 8. This is likely caused by a smaller discovery rate for *Kepler* at longer periods and therefore less training data at longer periods for all classes.

6.2. Comparison With Other Classification Algorithms

In addition to the random forest we also tried other classification algorithms, k-nearest neighbors (k-NN) and naive Bayes.

The k-NN algorithm (Duda et al. 2001) has the advantage that it is simple, explainable and provides bounded error, but in a different manner to the random forest. With training set of infinite size k-NN would converge to no more than twice the error bounds of a Bayesian classifier with perfect knowledge of the joint probability distribution function of all the attributes. k-NN classifies an unknown, x_u , as $\hat{y} = y_{j^*}$. j^* is computed using the minimum distance to some example in the training set as in the following equation,

$$j^* = \arg \min_{j \in \mathcal{L}} d(x_u, x_j). \quad (10)$$

Where d is the Euclidean distance function between points in the attribute space. We can broaden the no-

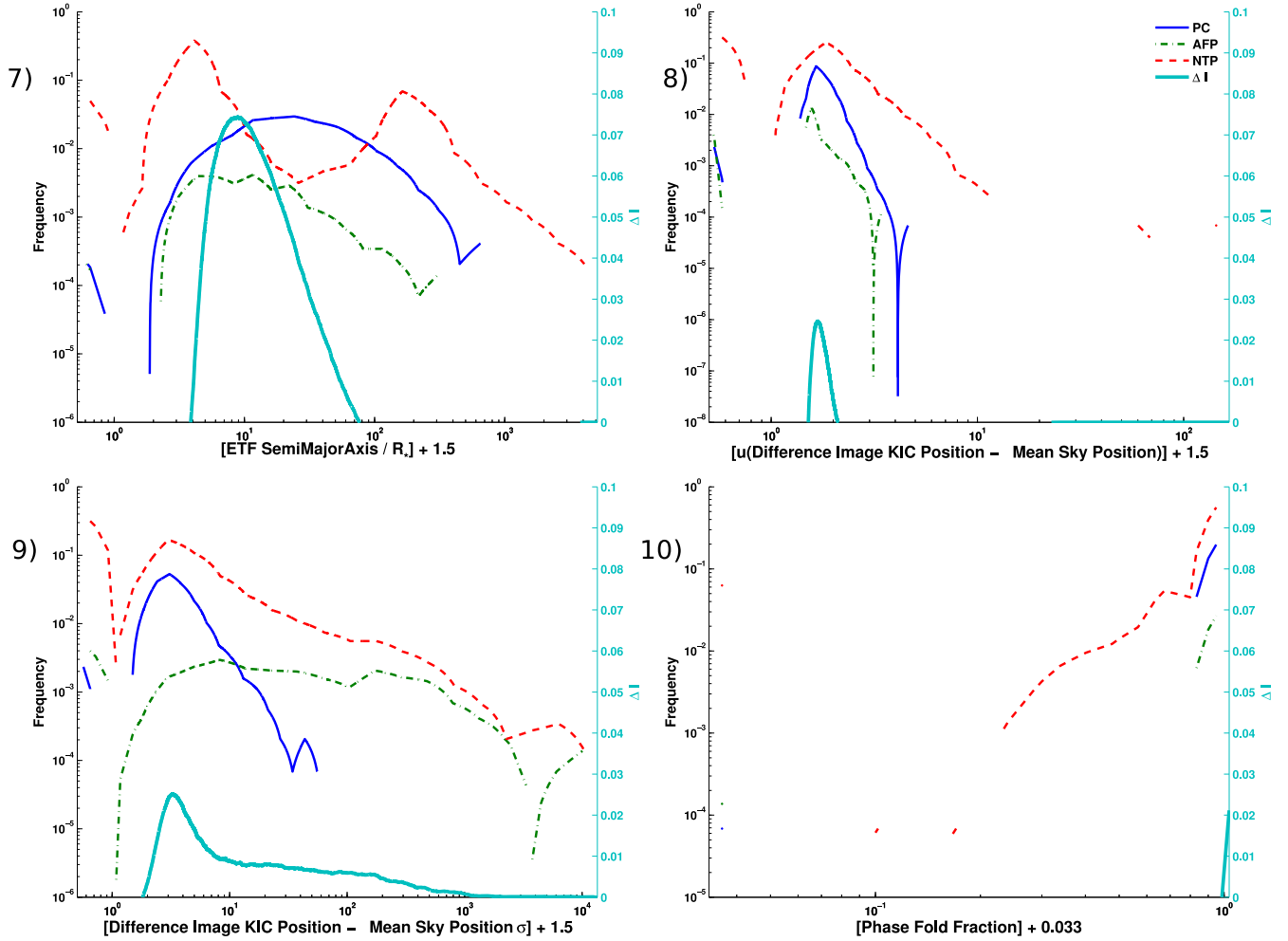


Figure 6. Class-conditional distributions of attributes 7 through 10. If an attribute’s domain extends to zero or negative numbers a small constant has been added so that it can be log scaled. ΔI (equation 2) is plotted to show where a split might be made if it was the first split in a decision tree.

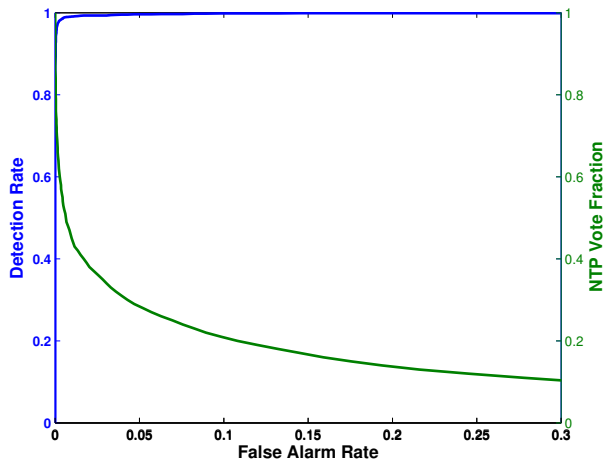


Figure 7. ROC curve for $(PC \cup AFP)$ vs NTP. $AUC = 0.9991 \pm 0.0004$

tion of distance in equation 10 to include the class of the k nearest neighbors instead of just the a single nearest neighbor, but for our problem the optimal k turns out to be $k = 1$. Other values of k turn out to have classification performance very close to random. An identical

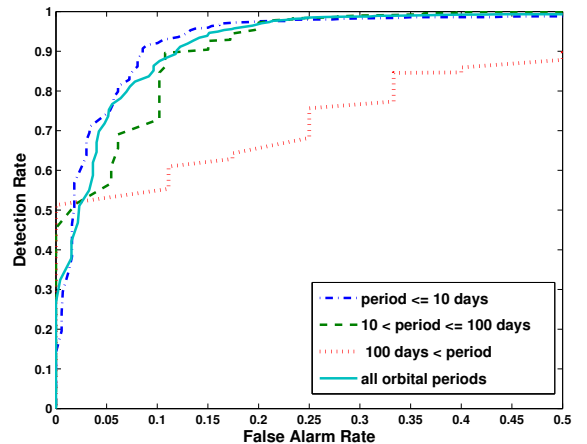


Figure 8. Period dependent ROC curve for PC vs AFP. For all orbital periods the AUC is 0.9522 ± 0.0080 . For the orbital period bins ($p \leq 10$, $10 < p \leq 100$, and $p > 100$) the AUC are 0.9568 ± 0.0094 , 0.9484 ± 0.0193 , and 0.8229 ± 0.0730 respectively.

training set is used for RF and k-NN except that the attributes are log scaled. To assess k-NN performance we use leave-one-out cross validation. Unfortunately, since

Table 3
k-NN confusion matrix

Training Set Class	Predicted Class		
	PC	AFP	NTP
PC	2,776	57	46
AFP	100	260	33
NTP	164	59	11,081

Table 4
Naive Bayes confusion matrix

Training Set Class	Predicted Class		
	PC	AFP	NTP
PC	2,718	95	66
AFP	168	210	15
NTP	32	22	11,250

$k = 1$, it's not possible to plot an ROC curve for k-NN since its classification space is just a single point. See figure 9.

A naive Bayes classifier assigns $\hat{y} = \mathbf{y}_{i^*}$ by choosing the class with the highest probability given the evidence.

$$i^* = \arg \max_i P(\mathbf{y}_i | x_u) \quad (11)$$

$$P(\mathbf{y}_i | x) = P(\mathbf{y}_i) \prod_{j=1}^A \frac{P(x_j | \mathbf{y}_i)}{P(x_j)}$$

Where x refers to the attributes of the unknown TCE and A is the number of attributes. Prior probabilities, $P(\mathbf{y}_i)$, of classes are estimated from the frequency of the classes in the training set. Probability distributions, $P(x_j | \mathbf{y}_i)$, are estimated using a kernel density estimator. We use a Gaussian kernel with Silverman's rule-of-thumb bandwidth described in Feigelson & Babu (2012). Implied by equation 11 is that our attributes are independent from one another; it is naive after all.

We use leave-one-out cross validation to estimate the classification performance. The resulting confusion matrices for k-NN and naive Bayes classifiers are presented in tables 3 and 4 respectively. Performance of all classification algorithms described in this paper are presented for the purpose of discriminating between $PC \cup AFP$ vs NTP in figure 9.

These results show that while other classification algorithms have better than random performance they do not perform as well as the random forest.

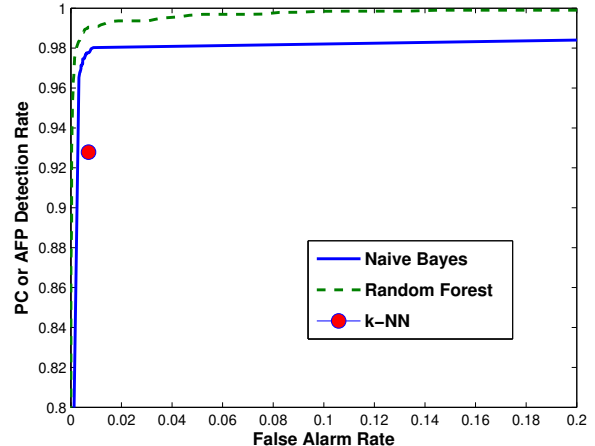


Figure 9. Comparison of random forest, naive Bayes and k-NN. AUC=0.9991 for random forest and 0.9894 for naive Bayes. k-NN (when $k = 1$) does not produce a ranking of predictions and so is represented as a single point in the trade space between detection rate and false alarm rate.

7. APPLICATION TO TRANSIT SURVEYS

7.1. Predictions on Later TCERT Dispositions

The TCE catalog contains 3,831 TCEs that are not labeled. Of these 1,487 have since been given dispositions by the TCERT. We look at the classification predictions that have been generated by the random forest on these 1,487 TCEs. Table 5 contains the confusion matrix of the random forest predictions.

Very few planet candidates are misclassified yielding a detection rate for PC on this set of TCEs of 86.4%. Precision is lower for planet candidates, only 62.2 % of TCEs classified as planet candidates are actually planet candidates for this set. We looked at a random sample of a small number of AFPs that were misclassified as PCs. The vast majority of these were determined by the TCERT to be AFPs based on information not available in the set of attributes. These dispositions are based on the presence of significant secondary eclipses, indicating an eclipsing binary. Another source of false positives is direct PRF contamination. In these cases the light from a nearby, but out-of-aperture star, is inducing a transit signal on the target star and our existing attributes are not able to detect the off aperture false positive. Some of these problematic TCEs are discussed in Coughlin et al. (2014)

7.2. Classifying Against Longer Orbital Periods Than Training Data

A transit survey such as *Kepler* will initially discover larger, shorter period planets. As the survey continues it will find smaller, longer period planets. This poses a potential issue to supervised machine learning algorithm as a portion of parameter space it is trained on may no longer be representative of the population as a whole.

Table 5
Random Forest Predictions

TCERT Class	Predicted Class		
	PC	AFP	NTP
PC	336	10	43
AFP	204	388	506

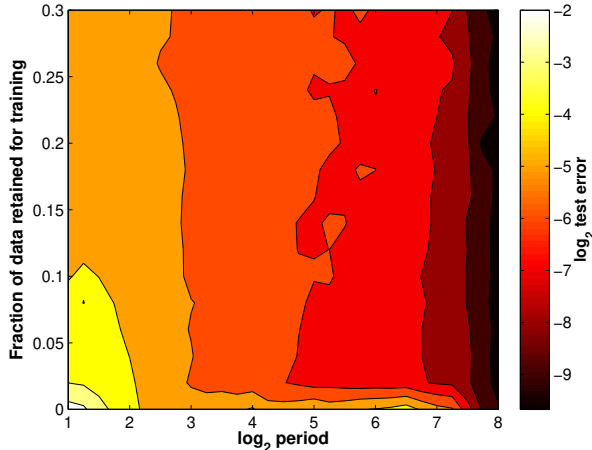


Figure 10. The effects of limiting the amount of training data used to less than some orbital period. The abscissa is the \log_2 orbital period. The ordinate is the portion of the TCEs retained for training that have orbital periods less than the abscissa. The value plotted is \log_2 of all the data that was not used for training.

We look at what happens to classification errors when we only have successively smaller amounts of training data and for shorter orbital periods.

Figure 10 shows the error rates achieved when limiting the training data used at various orbital period thresholds. The error is computed by training three random forests for each combination of period and threshold evaluated. The error for an individual random forest is then computed on the test set (the portion of the training data that was not used for training) and the OOB error. The mean error is used to estimate the error surface in figure 10.

At a period of 16 days and training data fraction of zero no training data longer than 16 days is used to train the random forests. The error rate for this orbital period is 3.13%. If we were then expanding our search to longer periods then we would only need to add 5% of the TCEs with periods longer than 16 days to have the error rates fall to 1.56%. Therefore adding a small, but uniformly sampled (with respect to orbital period) portion of the unknown TCEs to the training set can yield a large reduction in misclassification error.

8. CONCLUSION

Machine learning techniques offer a way to automate some stages of exoplanet discovery. In this paper we have demonstrated that the random forest algorithm is quite good at distinguishing between systematic noise, eclipsing binary and exoplanet candidate signatures. As seen in table 2, classifications have a low overall error rate (1.34%), exoplanet classifications have high precision (95.9%) and recall (98.7%) but not without some caveats.

When used to predict on longer orbital periods than the training data the overall error rate increases. This can be mitigated by sampling a small percentage of the more recent TCE detections, classifying them and adding them to the training set. There are some populations of astrophysical false positives that have been identified using other methods, information not available in the training dataset. The random forest often confuses these astrophysical false positive TCEs with planet candidates

and non-transiting phenomena (table 5).

In the future we intend on adding additional attributes that would help separate out the astrophysical false positives. Newer versions of the TPS software can detect weak secondary eclipses that would indicate the presence of an eclipsing binary. Transit signatures induced by off-aperture sources can be identified by performing photometry on the local background pixels of the target stars. Transits detected in this aperture should then not have similar significance to the transits detected on the target stars.

The *Kepler* mission is currently working on estimating the completeness of the pipeline using injected transits (Christiansen et al. 2013). Using injected transits as training data can be used to assess the accuracy of human and machine classification efforts. We look forward to continued revision and applications of these automated classification methods on subsequent *Kepler* pipeline runs, and these methods can be readily applied to large transit surveys in the future such as TESS (Ricker et al. 2014).

ACKNOWLEDGMENTS

We would like to thank Abhishek Jaiantilal for use of the randomforest-matlab code. This paper would not be possible without the work of the members of the *Kepler* TCE Review Team. Funding for the *Kepler* mission is provided by NASA’s Space Mission Directorate. This research has made use of the NASA Exoplanet Archive, which is operated by the California Institute of Technology, under contract with NASA under the Exoplanet Exploration Program.

REFERENCES

- Ballard, S., Fabrycky, D., Fressin, F., et al. 2011, *ApJ*, 743, 200
 Batalha, N. M., Borucki, W. J., Bryson, S. T., et al. 2011, *ApJ*, 729, 27
 Batalha, N. M., Rowe, J. F., Bryson, S. T., et al. 2013, *ApJS*, 204, 24
 Borucki, W. J., Koch, D. G., Basri, G., et al. 2011, *ApJ*, 736, 19
 Breiman, L. 2001, *Machine learning*, 45, 5
 Breiman, L., Friedman, J. H., Olshen, R. A., & Stone, C. J. 1984, *Classification and Regression Trees* (Wadsworth)
 Bryson, S. T., Jenkins, J. M., Gilliland, R. L., et al. 2013, *PASP*, 125, 889
 Burke, C. J., Bryson, S. T., Mullally, F., et al. 2014, *ApJS*, 210, 19
 Caldwell, D. A., Kolodziejczak, J. J., Van Cleve, J. E., et al. 2010, *ApJ*, 713, L92
 Christiansen, J. L., Clarke, B. D., Burke, C. J., et al. 2013, *ApJS*, 207, 35
 Claret, A., & Bloemen, S. 2011, *VizieR Online Data Catalog*, 352, 99075
 Coughlin, J. L., Thompson, S. E., Bryson, S. T., et al. 2014, *AJ*, 147, 119
 Dubath, P., Rimoldini, L., Süveges, M., et al. 2011, *MNRAS*, 414, 2602
 Duda, R. O., Hart, P. E. P. E., & Stork, D. G. 2001, *Pattern classification*, 2nd edn. (Wiley)
 Feigelson, E., & Babu, G. 2012, *Modern Statistical Methods for Astronomy: With R Applications* (Cambridge University Press)
 Jenkins, J. M., Caldwell, D. A., Chandrasekaran, H., et al. 2010a, *ApJ*, 713, L87
 Jenkins, J. M., Chandrasekaran, H., McCauliff, S. D., et al. 2010b, in *Proc. SPIE*, Vol. 7740, 77400D–1–77400D–12
 Liaw, A., & Wiener, M. 2002, *R News*, 2, 18
 Mandel, K., & Agol, E. 2002, *ApJ*, 580, L171
 Prša, A., Batalha, N., Slawson, R. W., et al. 2011, *AJ*, 141, 83
 Richards, J. W., Starr, D. L., Butler, N. R., et al. 2011, *The Astrophysical Journal*, 733, 10

- Ricker, G. R., Winn, J. N., Vanderspek, R., et al. 2014, arXiv preprint arXiv:1406.0151
- Seader, S., Tenenbaum, P., Jenkins, J. M., & Burke, C. J. 2013, ApJS, 206, 25
- Smith, J. C., Stumpe, C., Cleve, J. E. V., et al. 2012, PASP, 124, 1000
- Stumpe, M. C., Smith, J. C., Cleve, J. E. V., et al. 2012, PASP, 124, 985
- Tenenbaum, P., Jenkins, J. M., Seader, S., et al. 2013, ApJS, 206, 5
- Thompson, S. E., Everett, M., Mullally, F., et al. 2012, ApJ, 753, 86
- Wu, H., Twicken, J. D., Tenenbaum, P., et al. 2010, in Proc. SPIE, Vol. 7740, 774019–1–774019–12